

# 1-prong Tau Decays into Charged Kaons

M. Davier, H.J. Park  
LAL, Orsay

## 1 Introduction

The experimental information on Cabibbo-suppressed  $\tau$  decays is rather poor [1]. While the  $K^*$  channel is well measured through the  $K_S^0\pi$ ,  $K_S^0 \rightarrow \pi^+\pi^-$  mode [2]

$$B_{K^*} = (1.42 \pm 0.18)\% \quad (WA)$$

the situation is much worse for the other one-prong decays :

$$\begin{aligned} B_{K+\geq 0 \text{ neutrals}} &= (1.68 \pm 0.24)\% \quad (WA) \\ B_K &= (0.67 \pm 0.23)\% \quad (WA) \end{aligned}$$

In particular, the precision of the last result is not sufficient to significantly test this sector of the hadronic  $\tau$  current, through  $K \rightarrow \mu\nu$  and  $\mu - \tau$  universality.

The situation could also be complicated by the presence of small, but badly known (or even unknown altogether) Cabibbo-allowed modes with kaons, such as  $K\bar{K}(\pi\dots)$  channels. A precise analysis of the  $\tau$  strange sector will certainly have to face this problem.

In this note, we present a measurement with ALEPH of the one-prong charged kaon  $\tau$  decay rate, i.e.

$$\tau^- \rightarrow \nu_\tau K^- + \geq 0 \text{ neutrals}$$

where the neutrals include  $\pi^0$ 's and  $K^0$ 's. The dominant branching fractions for the channels

$$\tau^- \rightarrow \nu_\tau K^-$$

$$\tau^- \rightarrow \nu_\tau K_{\rightarrow K-\pi^0}^{*-}$$

and

$$\tau^- \rightarrow \nu_\tau K^- \pi^0 \pi^0$$

are extracted, after subtracting contributions from small modes ( $\tau^- \rightarrow \nu_\tau K^- K_L^0$ ,  $\tau^- \rightarrow \nu_\tau K^- \pi^0 K_L^0$ ) measured with an independent analysis [3]. In this analysis, the charged kaons are identified by  $dE/dx$  in the TPC, through a calibration procedure almost completely based on data.

## 2 Event Selection

Events are selected using the  $\tau^+\tau^-$  TAUSLT filter, an improved version of the earlier program described in [4]: its overall efficiency is 77.1% including the geometrical acceptance, while the background is reduced to only 1.3%, affecting mostly the leptonic decays (from  $Z \rightarrow e^+e^-$ ,  $\mu^+\mu^-$ , and  $\gamma\gamma \rightarrow leptons$ ) and to a lesser extent the multi-prong decays (from  $Z \rightarrow q\bar{q}$ ).

Decays with only one 'good' track ( $\geq 4$  TPC pads,  $|d_o| < 2cm$ ,  $|z_o| < 10cm$ ) are kept with the following further requirements:

- $P > 2$  GeV
- identification as a hadron by TAUPID [5]

Note that TAUPID uses  $dE/dx$  in the process of  $e/\mu/h$  separation, but this introduces a negligible bias in this analysis because of the small weight of  $dE/dx$  compared to the other estimators (except for  $e$  identification) and also because  $\pi$  distributions are used in the program for hadrons (the value of  $dE/dx$  for kaons being further away from that of  $e$ 's and  $\mu$ 's, the contamination in a  $K$  sample is expected to be very small,  $\ll 1\%$ ).

Photons are reconstructed with GAMPEX, with a threshold of 250 MeV, and  $\pi^0$ 's are identified as usual ( $0.07 < m_{\gamma\gamma} < 0.21$  GeV). This allows the decay data sample to be split in 4 classes:

$$\begin{aligned} \text{'h inclu'} &\equiv h + \geq 0\gamma \\ \text{'h'} &\equiv h + 0\gamma \\ \text{'h}\pi^0 &\equiv h + 1\pi^0 \text{ or } 1\gamma \text{ with } E > 4 \text{ GeV} \\ \text{'h}2\pi^0 &\equiv h + 2\pi^0 \text{ or } 1\pi^0 + 1\gamma \text{ with } E_\gamma > 4 \text{ GeV or } 2\gamma \text{ each with } E_\gamma > 4 \text{ GeV} \end{aligned}$$

Data from 91 and 92 are used, yielding a sample of 28481 one-prong  $\tau$  candidates, of which 28390 have  $dE/dx$  information.

### 3 Method

The measured  $dE/dx$  deposit ( $R$ ) is to a very good approximation gaussian-distributed around the expected value, computed from the Bethe-Bloch formula [6]. Each track is assigned a probability density according to the measured  $R$  and depending on the assumed particle type  $i$  ( $i=\pi, K$ ), giving a kaon probability

$$P_K = \frac{W_K(R)}{W_K(R)+W_\pi(R)}$$

To first order,  $W_i(R)$  is gaussian and therefore determined by its mean  $\overline{R}_i$  and its standard deviation  $\sigma_i$ . These are given by the QDEDX routine, taking into account the energy loss process and well-known geometrical effects (angle-dependent number of samplings, and cracks between TPC sectors).

However, this is not enough for our purpose, because a precise and reliable knowledge of  $W_{\pi,K}(R)$  is needed and therefore a detailed recalibration has to be undertaken using tracks from data :

$\mu\mu$  (45 GeV)

*minimum – ionizing pions* from  $q\bar{q}$  (0.4 – 0.6 GeV)

$\tau \rightarrow \mu$  (2 – 45 GeV)

$\tau \rightarrow h$  (2 – 45 GeV)

In the latter cases, it is important to take into account the contributions from mis-identified particles ( $\pi$  in  $\mu$  sample,  $e$  and  $\mu$  in  $h$  sample). Their rate is known from the detailed TAUPID studies which have been performed [5].

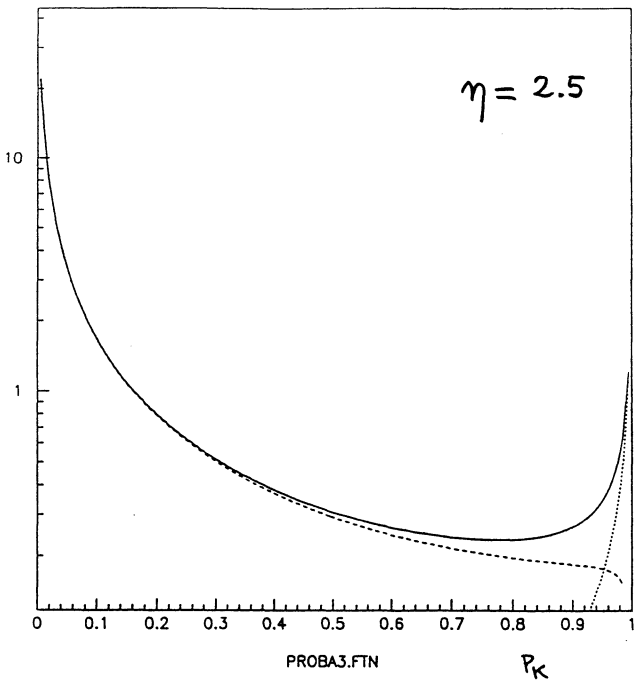
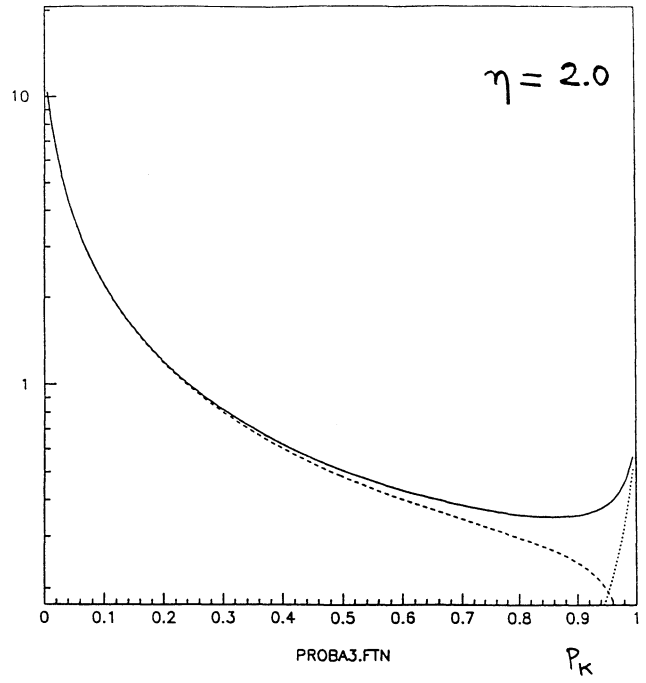
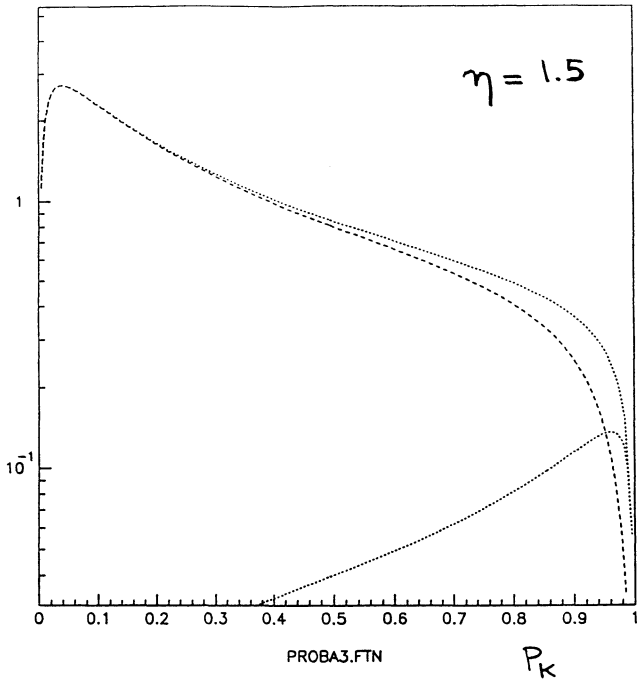
Finally, non-gaussian corrections to  $W_i(R)$  are determined and applied to the final probability densities.

The sensitivity of this method to a  $K$  signal depends crucially on the separation parameter

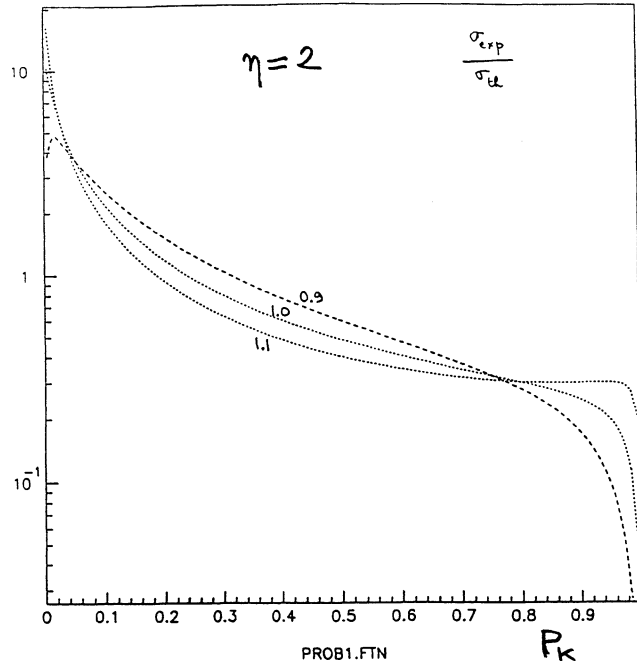
$$\eta = \frac{\overline{R}_\pi - \overline{R}_K}{\sqrt{\frac{1}{2}(\sigma_\pi^2 + \sigma_K^2)}}$$

The  $P_K$  probability distributions are given in Fig.1 for a gaussian  $W_i(R)$  and for 3 values for  $\eta$  : clearly a good identification requires  $\eta$  values in excess of 2. This will be the case in this analysis over most of the momentum range from 2 to 45 GeV.

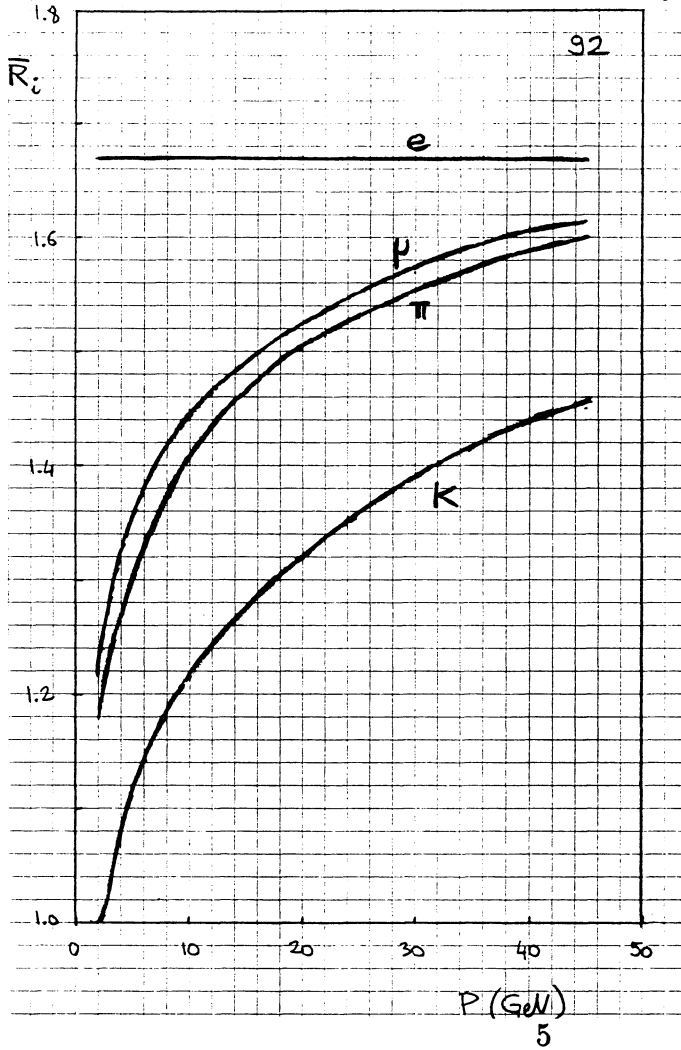
One could worry about the possibility to generate a fake  $K$  signal by using incorrect probability densities : such a possibility is explored in Fig.2 where the theoretical width of the  $W_i$  distribution used in the calculation of  $P_K$  is taken to be different from the real one. It shows that it is very important to fit the shape of the whole spectrum and not only the region near 1 : only then can one limit possible systematic biases.



1. Probability distributions calculated with gaussian probability densities  $W_{\pi,K}(R)$  for 3 values of the separation parameter  $\eta$ .



2. Probability distributions for a pure sample of pions calculated with a gaussian  $W_\pi(R)$  of standard deviation  $\sigma_{th}$ , whereas the 'data' distribution has a standard deviation  $\sigma_{exp}$ .



3. The range in  $\bar{R}$  values for 92 data.

## 4 Calibration of $dE/dx$

The relative range in  $\bar{R}$  is given in Fig.3 for 92 data. As outlined in the previous section, the strategy used for calibration is exclusively based on data. It is well-known that the observed  $R$  distributions show some important deviations from the expected ones : most notably, a  $\theta$  dependence of  $R$  is observed, mostly in 91 data and  $\sigma_{data}$  is about 10% smaller than  $\sigma_{expected}$ .

The following calibration procedure is applied separately for 91 and 92 data :

(a) a gaussian fit in each  $\theta$  bin yields  $\bar{R}(\theta)$

(b) the shift  $\bar{R}(\theta) - R_{expected}$  is fitted with polynomials as a function of  $\theta$  and  $R_{expected}$ (Fig.4) to yield the corrected value  $R_{corr}$ . In fact the  $\theta$  dependence is closely related to the number of samplings which could actually provide a better parameterization (this is being studied for further analyses).

(c) following the previous correction,  $\sigma_{corr}$  is then determined as a ratio of the observed width to  $\sigma_{expected}$  as a function of  $R_{expected}$

(d) finally, the normalized density distribution is checked for possible deviations from a gaussian form : a slight asymmetry is found which can be accounted for by modifying the argument of the exponential with 2 additional parameters (Fig.5).

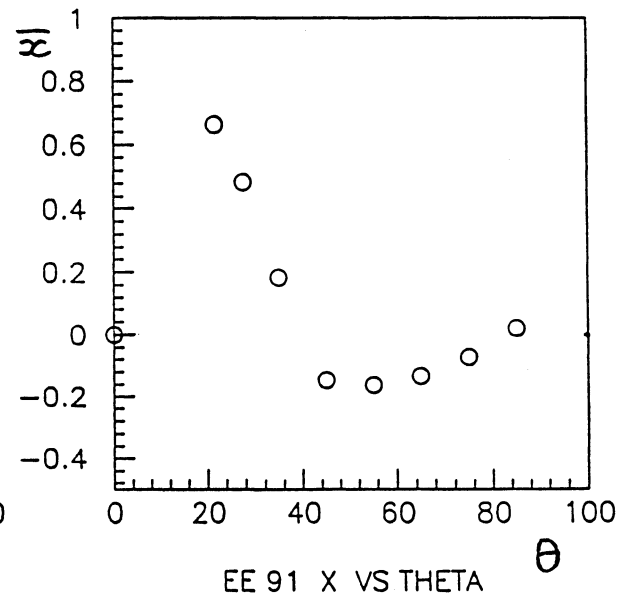
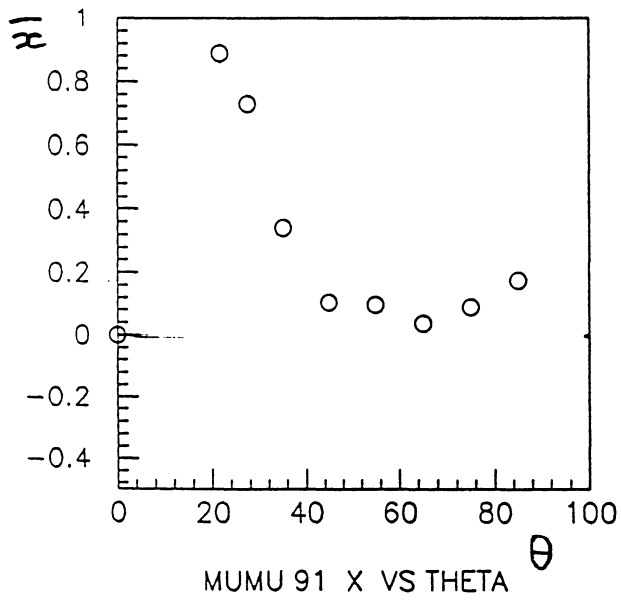
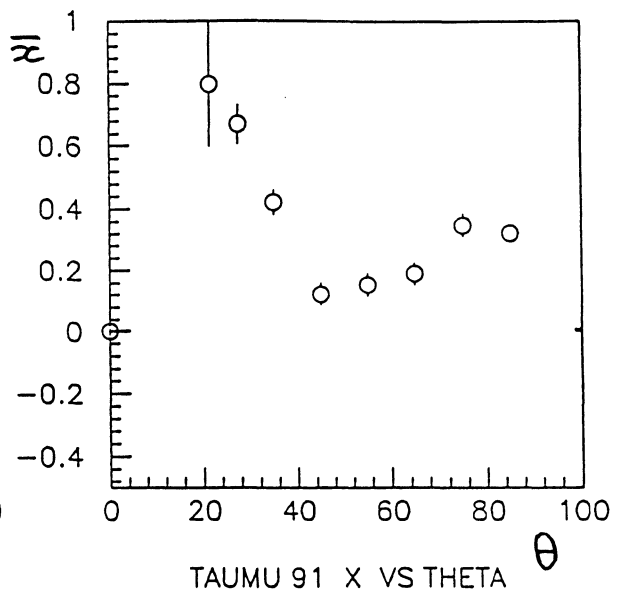
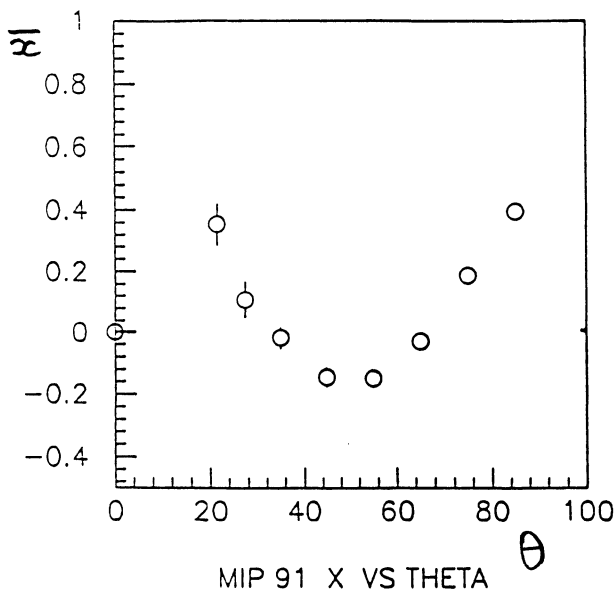
The final results given here differ from the preliminary values given last July by a small change in step (b) to take better into account the  $R$  dependence at the lowest pion momenta and by the use of a different modified gaussian (the previous form was not positive in all the ranges of parameters, giving some bias in the final likelihood fit).

The achieved  $K - \pi$  separation is given in Fig.6 .

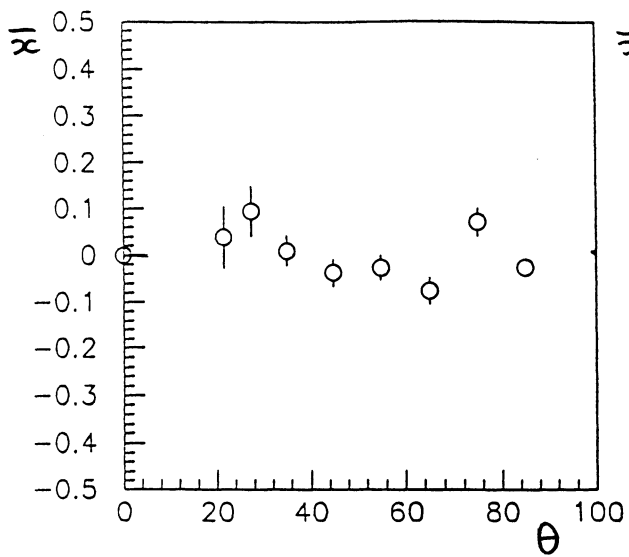
## 5 Fits

Although the presence of  $\mu/e$  contaminations in the hadron sample does not in practice affect the measurement of the  $K$  fraction, they are included in the fit to achieve an overall description of the  $dE/dx$  distribution, which is important as emphasized in Section 3. The contaminations are given by TAUPID and have been thoroughly checked with real data [5].

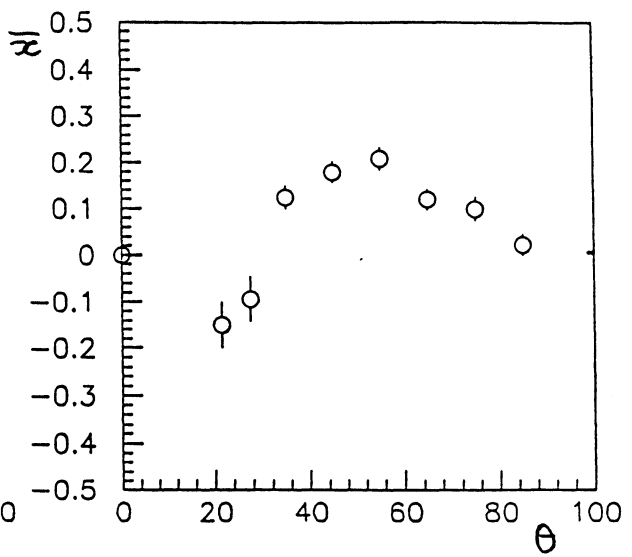
The  $dE/dx$  fits are done using either a likelihood method (MINUIT or a simpler home-made program) or a binned  $\chi^2$  fitting of the  $dE/dx$  distributions. The results are completely consistent in all cases, however, the errors delivered by MINUIT were found to be overestimated. Direct checks of the statistical error could be done using samples defined with a  $K$  probability cut. Final results are given with the binned



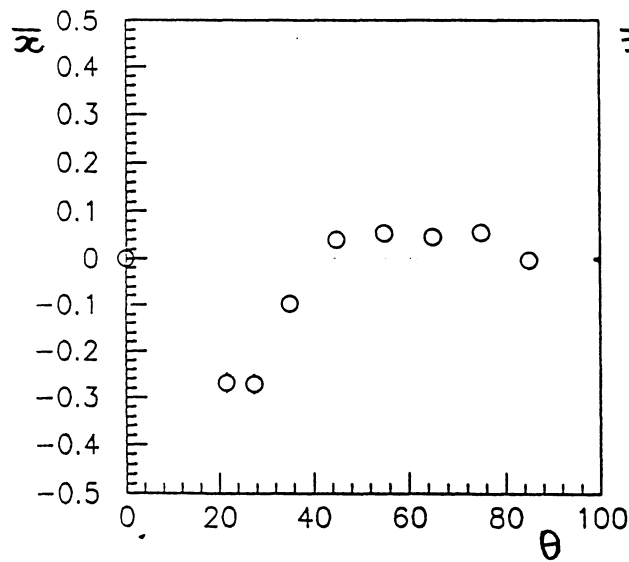
4. The shift in the mean  $dE/dx$  value as a function of  $\theta$ , measured through  $\bar{x}(\theta) = (\bar{R} - R_{expected})/\sigma_{expected}$  : (a) 91 data



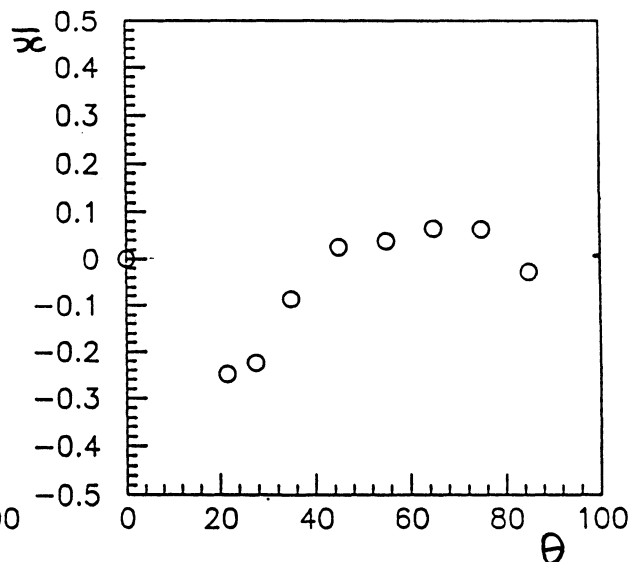
MIP 92 X VS THETA



TAUMU 92 X VS THETA



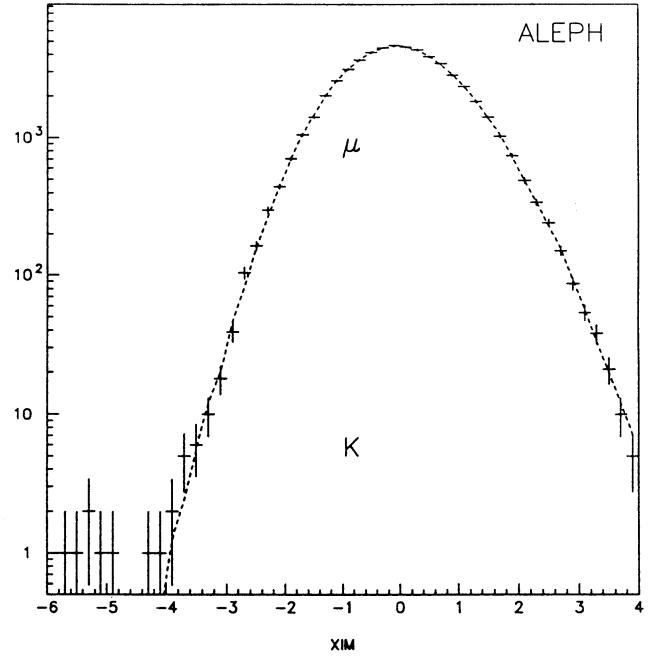
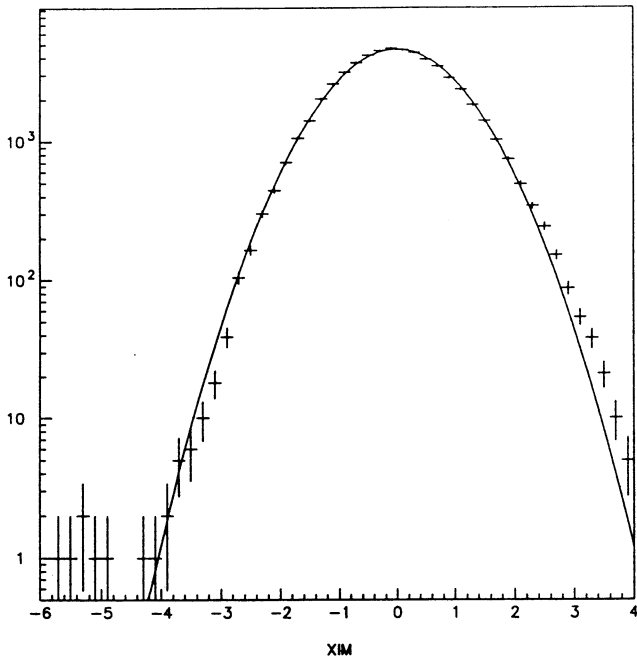
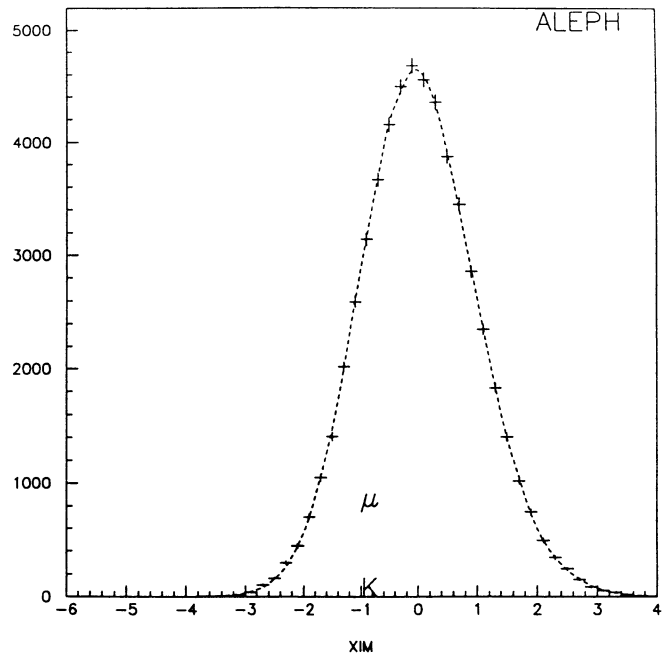
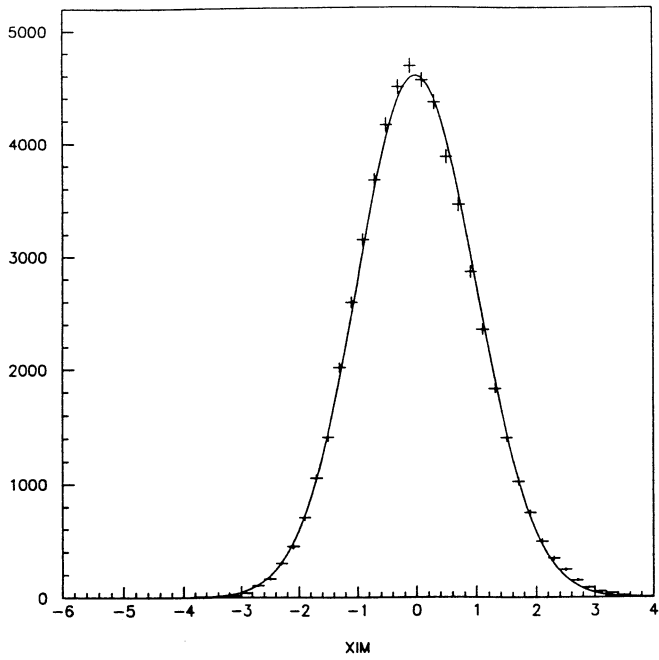
MUMU 92 X VS THETA



EE 92 X VS THETA

4. The shift in the mean  $dE/dx$  value as a function of  $\theta$ , measured through  $\bar{x}(\theta) = (\bar{R} - R_{expected})/\sigma_{expected}$  : (b) 92 data .



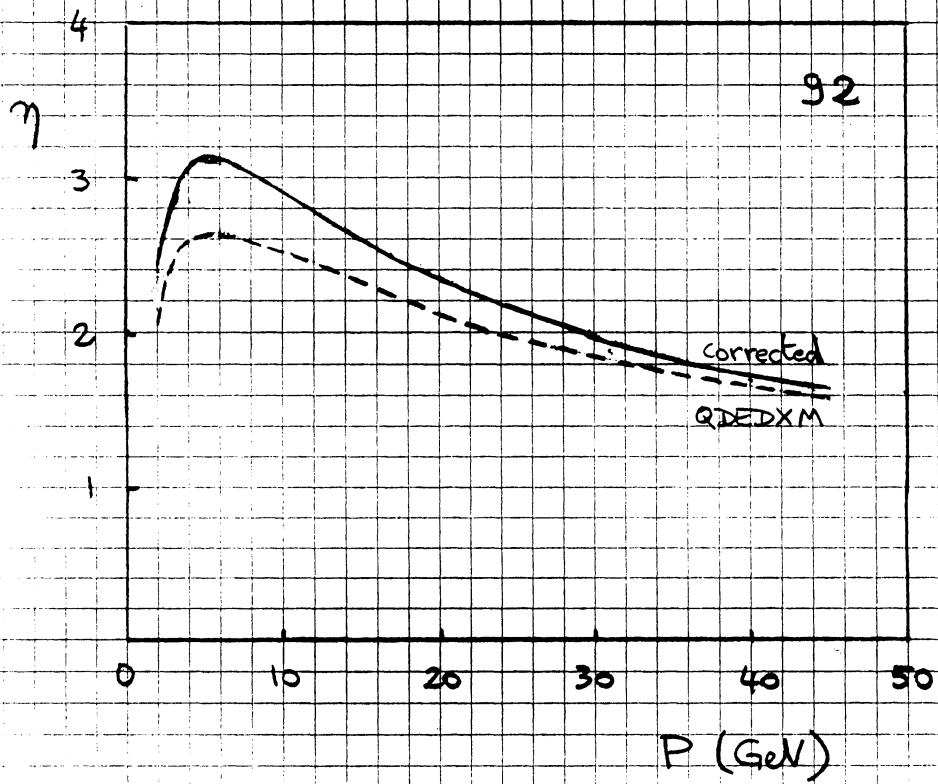
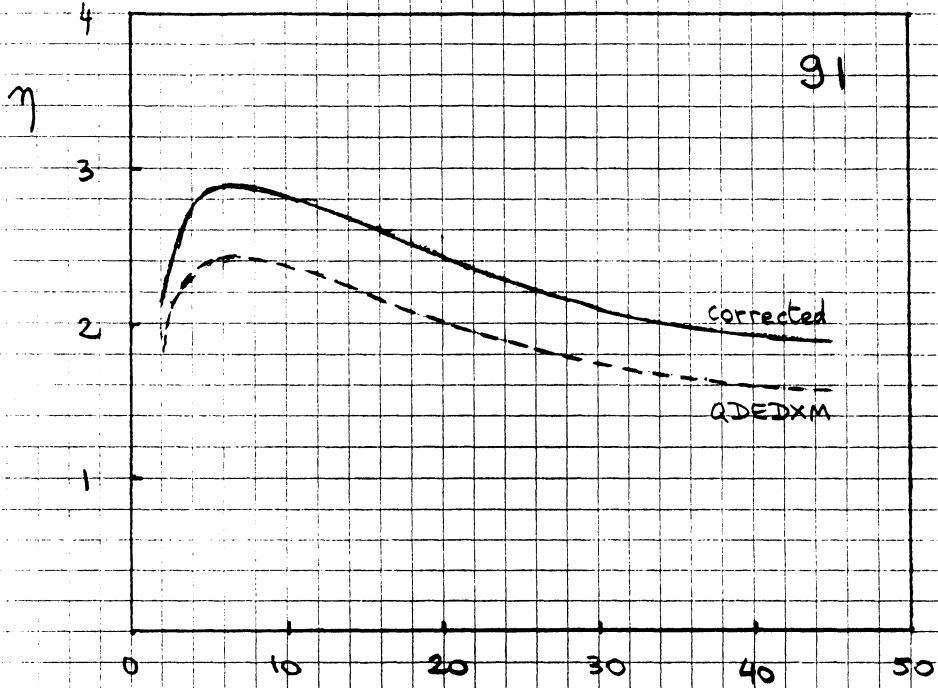


(a)

(b)

5. Fit to  $x$  distribution in  $Z \rightarrow \mu\mu$  events : (a) gaussian, (b) modified gaussian

$\pi$ -K SEPARATION



6. Achieved  $K - \pi$  separation for 91 and 92 data.

$\chi^2$  method as it can be more easily applied to cases where the  $K$  fraction is close to zero.

The results of the fits for the different data samples are given in Figs.7-11.

The main source of uncertainty is the reliability of the description of the  $\pi dE/dx$  distribution as a function of momentum. From likelihood fits with 3 parameters ( $K$  fraction  $f_K$ , deviation  $\Delta R$  from  $\pi$  corrected mean value  $R_{corr}^\pi$ , ratio  $\lambda$  of the width to the  $\pi$  corrected width  $\sigma_{corr}^\pi$ ), an overall check can be obtained with the inclusive hadron data :

$$\begin{aligned}\Delta R &= -0.00072 \pm 0.00084 \\ \lambda &= 1.0014 \pm 0.0097\end{aligned}$$

These values can be translated into a systematic effect on the  $f_K$  determination. However, a direct and more complete check is obtained from fitting a hypothetical  $K$  fraction in the  $\mu$  samples. The results in Table 1 and Fig.12 are the ingredients used for bounding possible systematic effects through convolution with the  $\pi$  momentum spectrum in each sample.

Table 1: *Estimate of systematic uncertainties*

sample	$h$ inclusive	$h$	$h\pi^0$	$h2\pi^0$
MC stat.(%)	1.7	2.7	3.5	7.1
selection+purity(%)	2	3	4	4
$dE/dx$ fit ( $\Delta f_K$ )	0.0022	0.0022	0.0023	0.0023

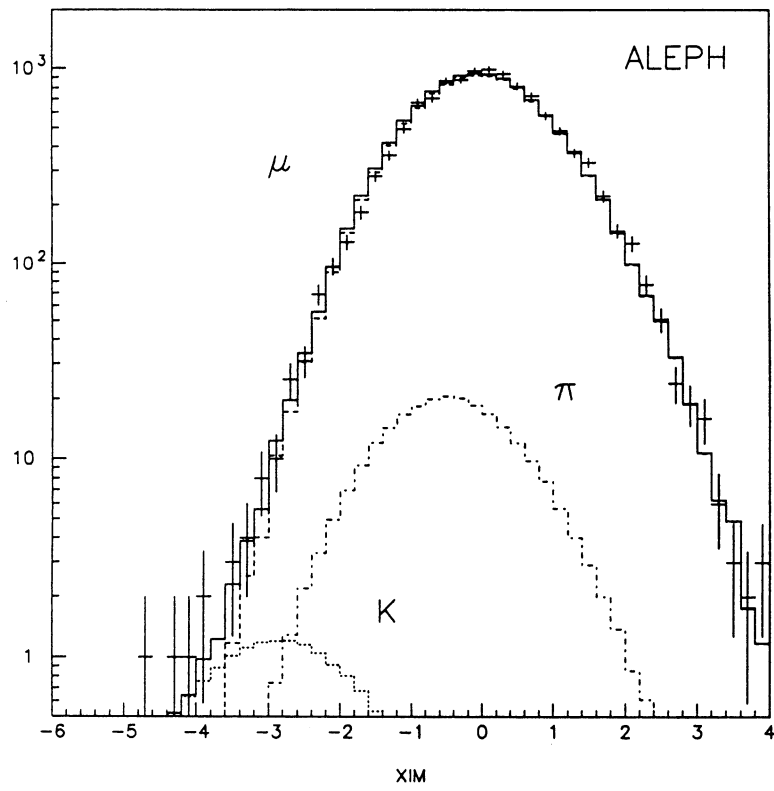
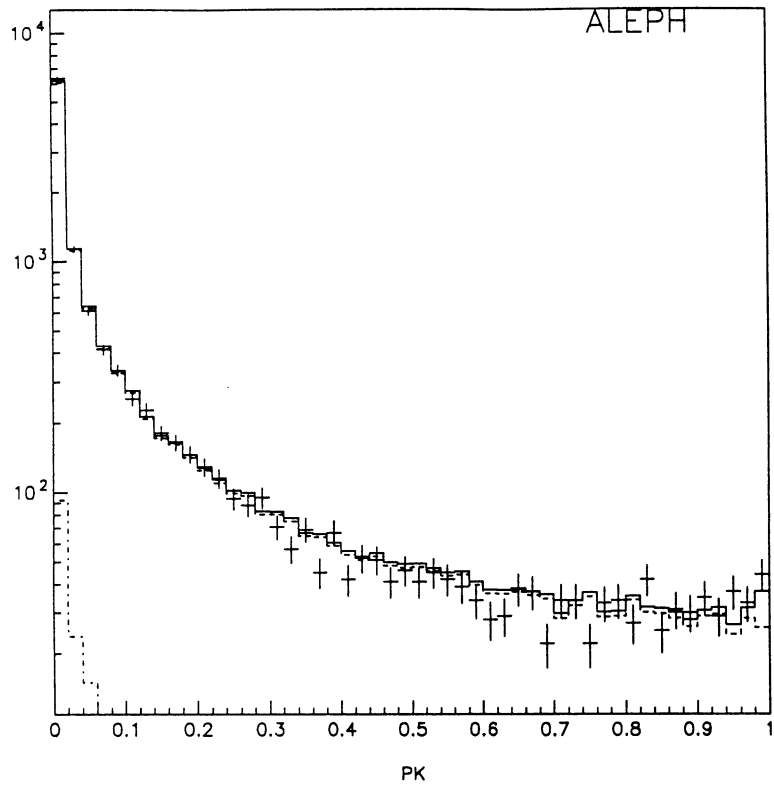
Some additional checks are possible :

(a) the  $K$  fraction is expected to vanish below the kinematical threshold of 3.6  $GeV/c$  (except for a very small contribution from radiative events). The result for the range 2-3.5  $GeV/c$  is consistent with expectation :

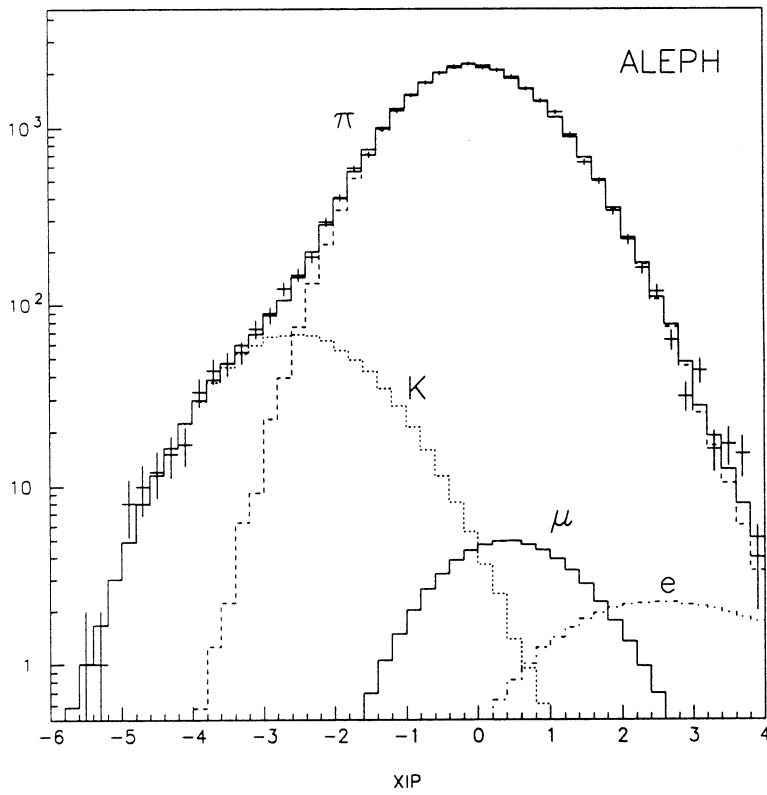
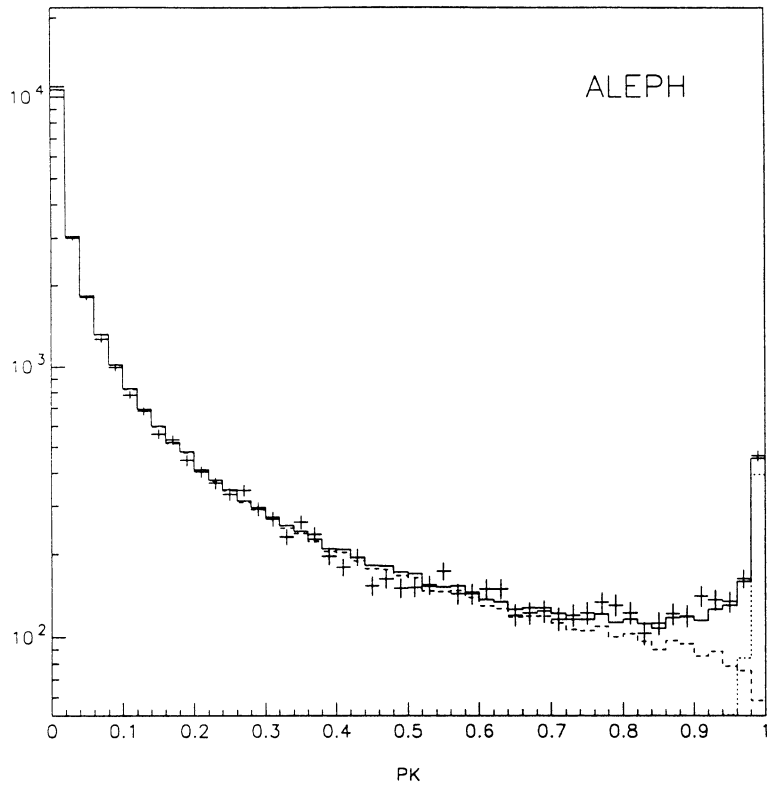
$$\begin{aligned}f_K &= (0.08 \pm 0.34)\% \\ f_K^{MC} &= (0.05 \pm 0.03)\%\end{aligned}$$

(b) the  $K\pi^0$  channel is expected to be dominated by the  $K^*(892)$  resonance which has a smaller  $Q$  value compared to the  $\rho \rightarrow \pi\pi^0$ . A cut below  $m_{K\pi} = 1 GeV$  isolates most of the  $K$  sample, a fact which is well satisfied experimentally (Fig.13) :

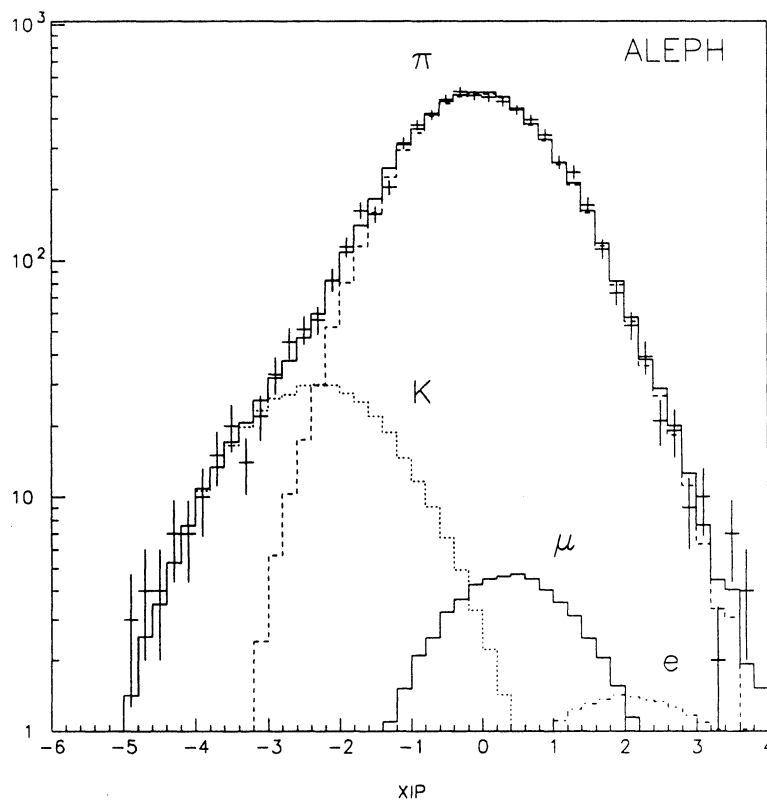
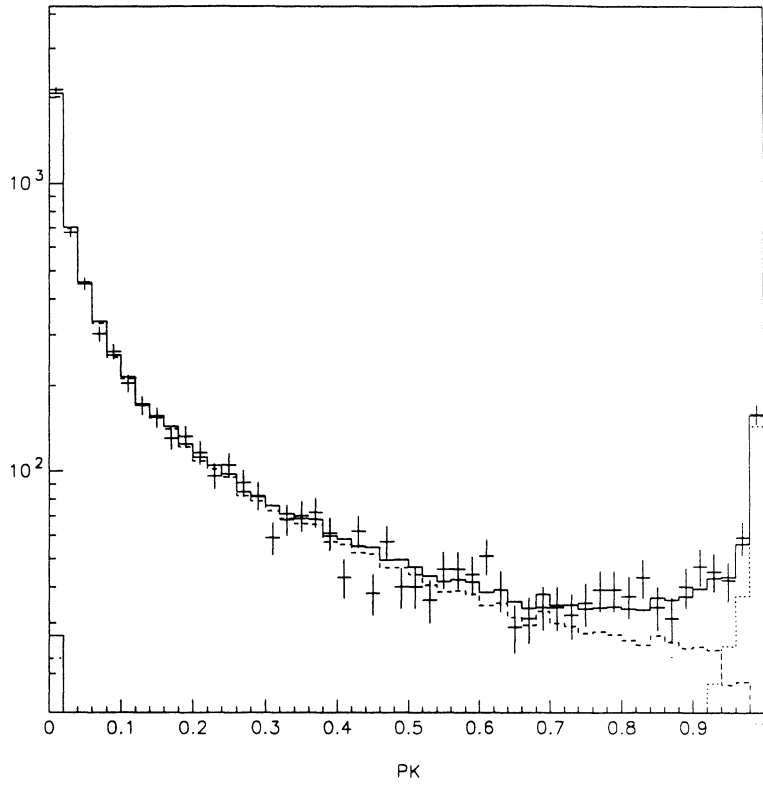
$$\begin{aligned}m_{K\pi} < 1GeV & \quad f_K = (5.24 \pm 0.48)\% \\ & \quad f_K^{MC} = (4.42 \pm 0.15)\% \\ m_{K\pi} > 1GeV & \quad f_K = (0.42 \pm 0.14)\% \\ & \quad f_K^{MC} = (0.38 \pm 0.04)\%\end{aligned}$$



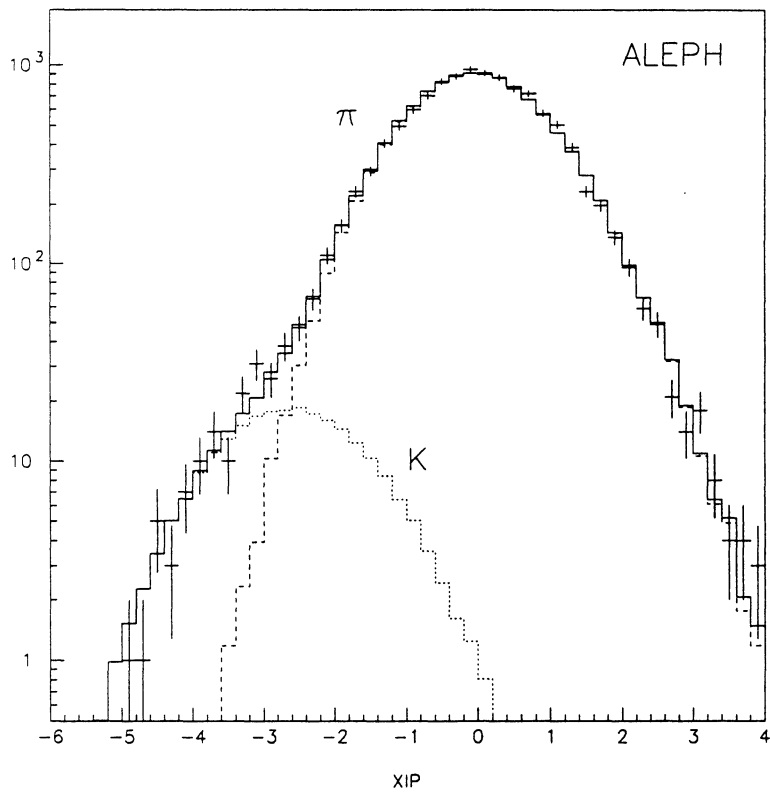
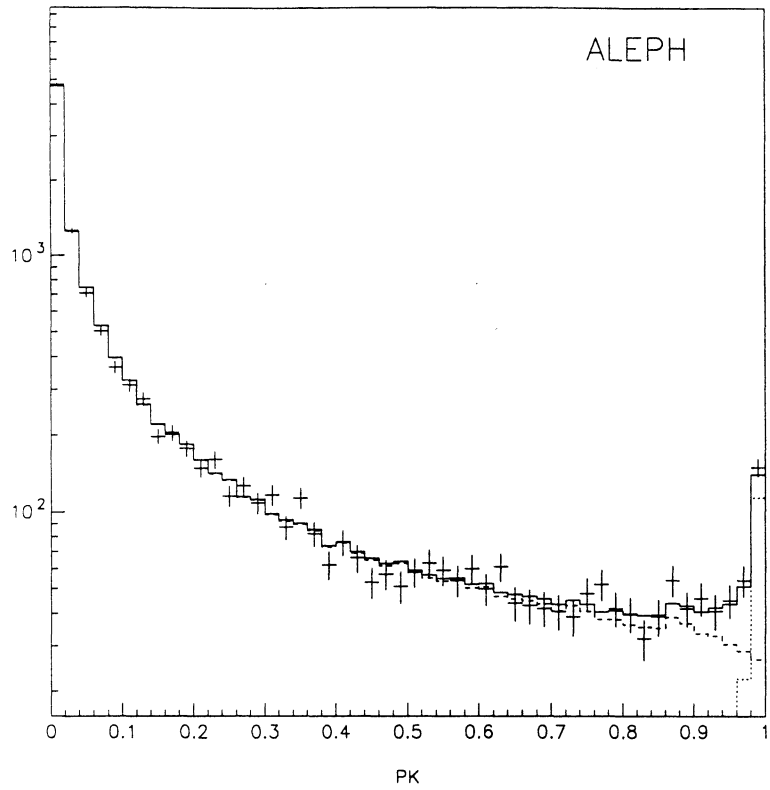
7. Fit to  $x_\mu$  distribution in  $\tau \rightarrow \nu_\tau \mu \bar{\nu}_\mu$  events.



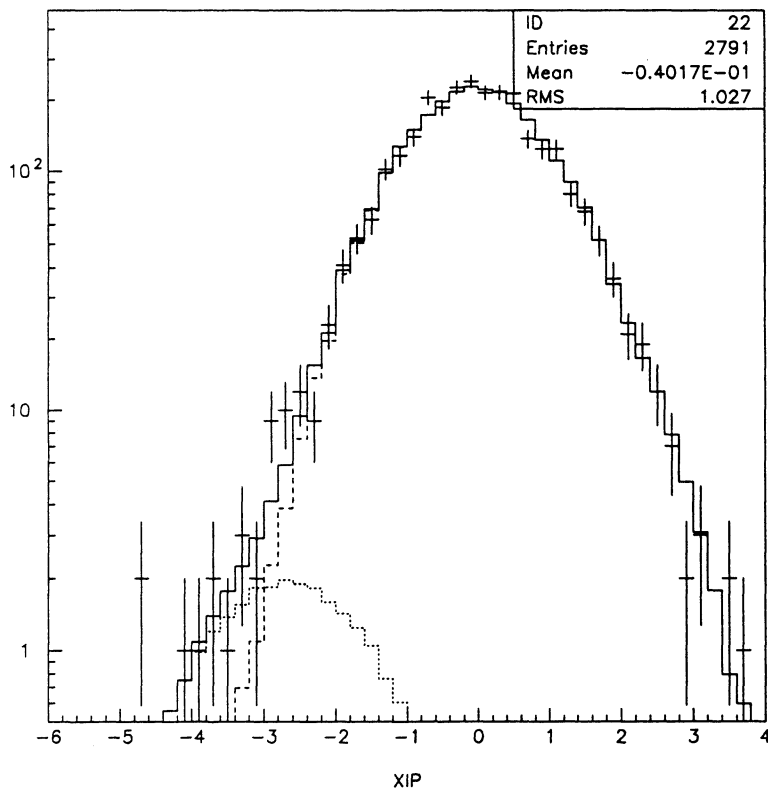
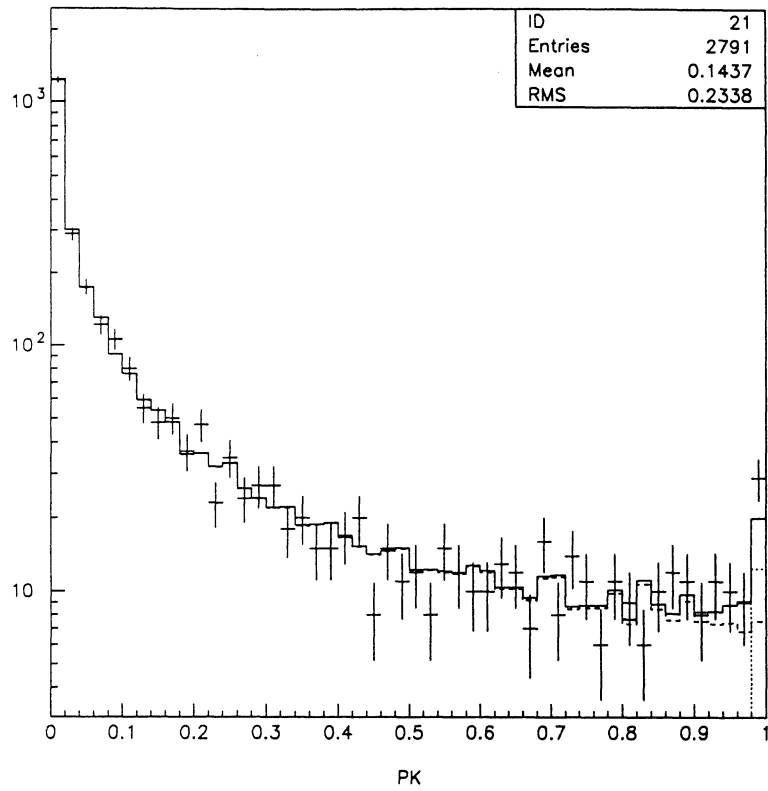
8. Fit to  $x_\pi$  distribution in  $h$  inclusive sample.



9. Fit to  $x_\pi$  distribution in  $h$  sample.

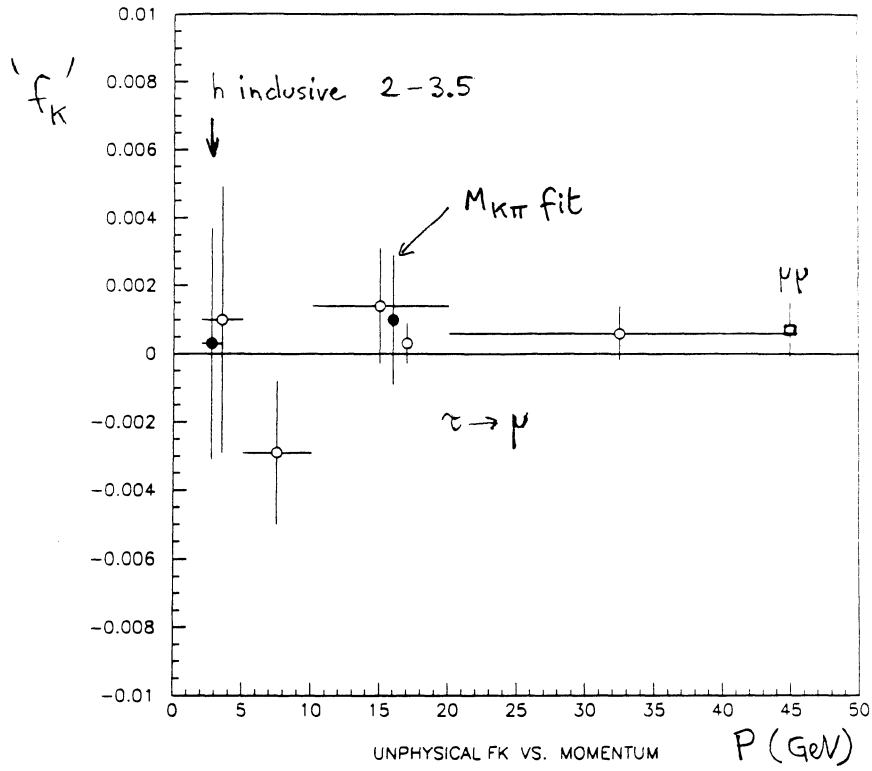


10. Fit to  $x_\pi$  distribution in  $h\pi^0$  sample.

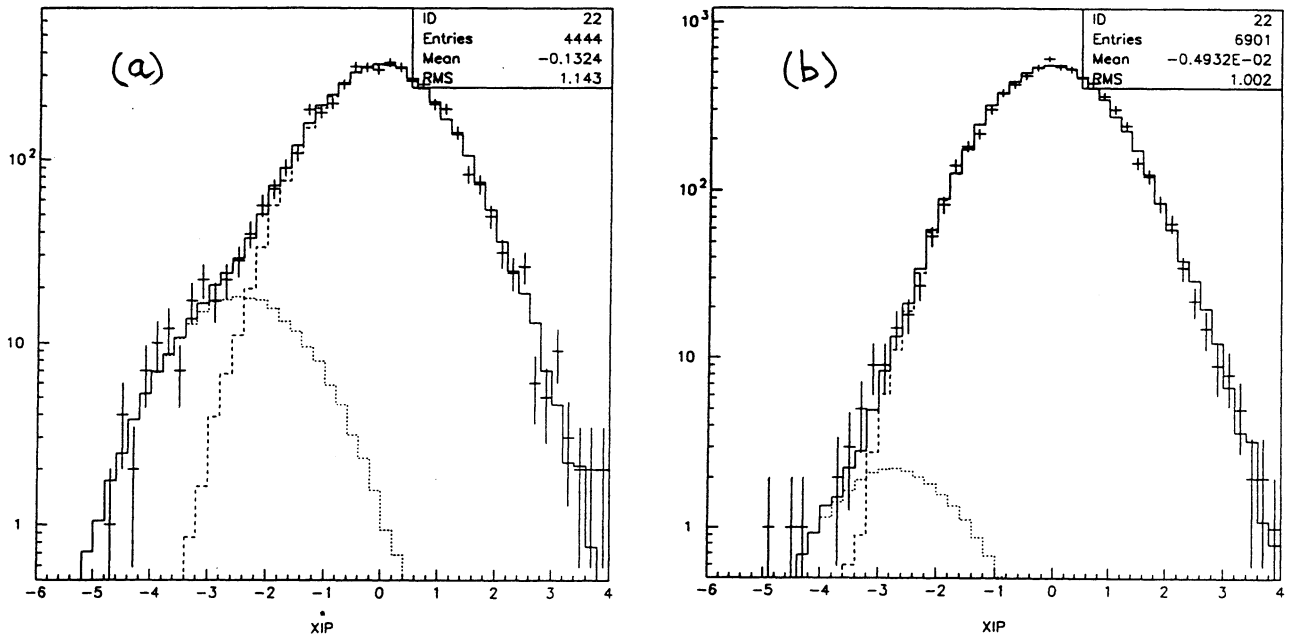


11. Fit to  $x_\pi$  distribution in  $h2\pi^0$  sample.





12. Unphysical  $f_K$  values to estimate global systematic uncertainties.



13. Fit to  $x_{\pi}$  distribution in  $h\pi^0$  sample : (a)  $m_{K\pi} < 1$  GeV (b)  $m_{K\pi} > 1$  GeV.

More quantitatively, one can estimate the  $\pi$  contamination in the fitted  $K$  sample using the experimental  $m_{K\pi}$  distribution and Monte Carlo distributions for  $K\pi^\circ$  and  $\pi\pi^\circ$  channels. The result

$$f_\pi = (4.8 \pm 9.6)\%$$

is indeed consistent with zero.

## 6 Results

As the selection procedure involves only 1 'good' charged track and photon requirements, it is possible that additional  $K^\circ$ 's be produced. In this case, the contamination is mostly from  $K_L^\circ$ 's and undecayed  $K_S^\circ$ 's (interacting in ECAL and HCAL), while  $K_S^\circ$  decays to  $\pi^\circ\pi^\circ$  are retained and  $K_S^\circ$  decays to  $\pi^+\pi^-$  are essentially removed by the track multiplicity cut. These various contributions can be estimated with KORAL06. However, since the absolute rate is not known from experiment, it is preferable to directly search for these channels in the  $K_L^\circ$  mode using HCAL, a procedure which is completely orthogonal with the present analysis based on tracks(TPC) and photons(ECAL). The  $K_L^\circ$  analysis is given separately [3] and provides results on the decay modes

$$\begin{aligned} \tau^- &\rightarrow \nu_\tau h^- K^\circ \\ &\nu_\tau h^- \pi^\circ K^\circ \end{aligned}$$

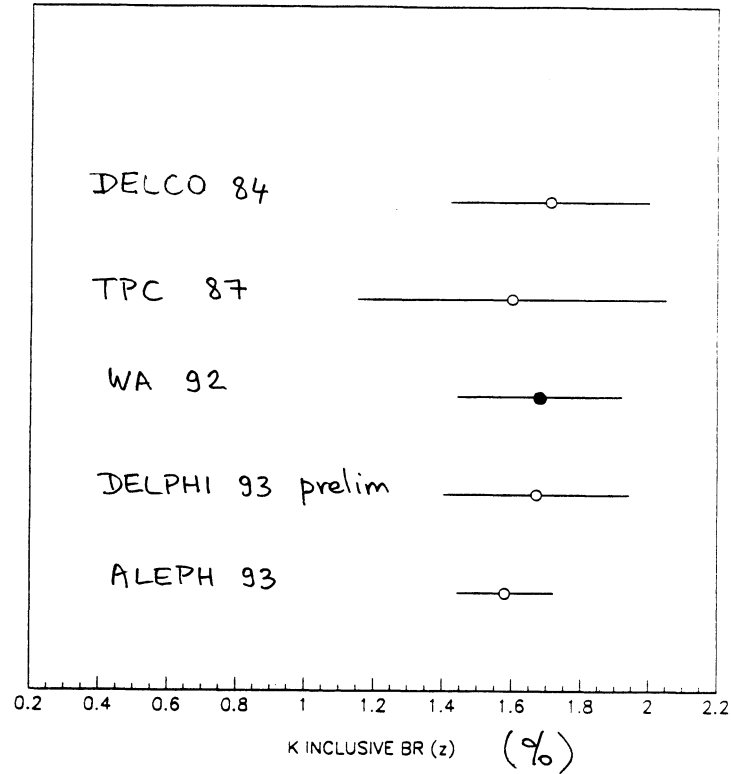
The contributions of the  $K^-K^\circ$  and  $K^-\pi^\circ K^\circ$  channels into the event samples used in the present analysis are computed using the Monte Carlo simulation, normalized to the measured total rate. The corresponding values are used to correct the measured branching ratios.

The final results are given in Table 2. For each channel, the efficiency and the background subtraction are computed from the Monte Carlo apart from the total rate of the  $K^-K^\circ$  (not included anyway in KORAL06) and  $K^\circ\pi^\circ K^\circ$  channels taken from the  $K_L^\circ$  analysis. The last branching ratio values given in the Table refer to well-defined final states with  $K^\circ$  corrections applied.

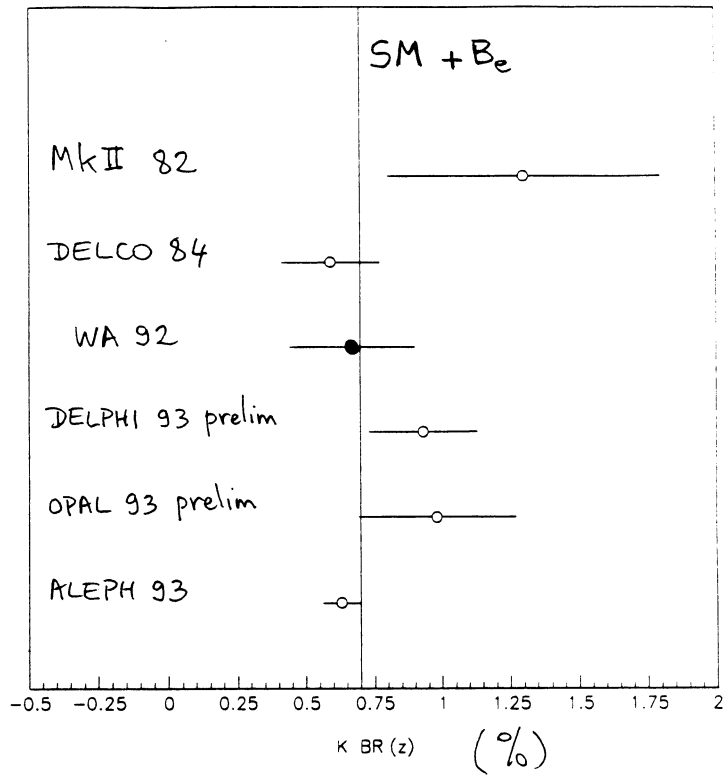
The inclusive rate agrees well with the previous world average, but it is more precise by almost a factor of 2 (Fig.14).

Table 2: Final results on branching fractions

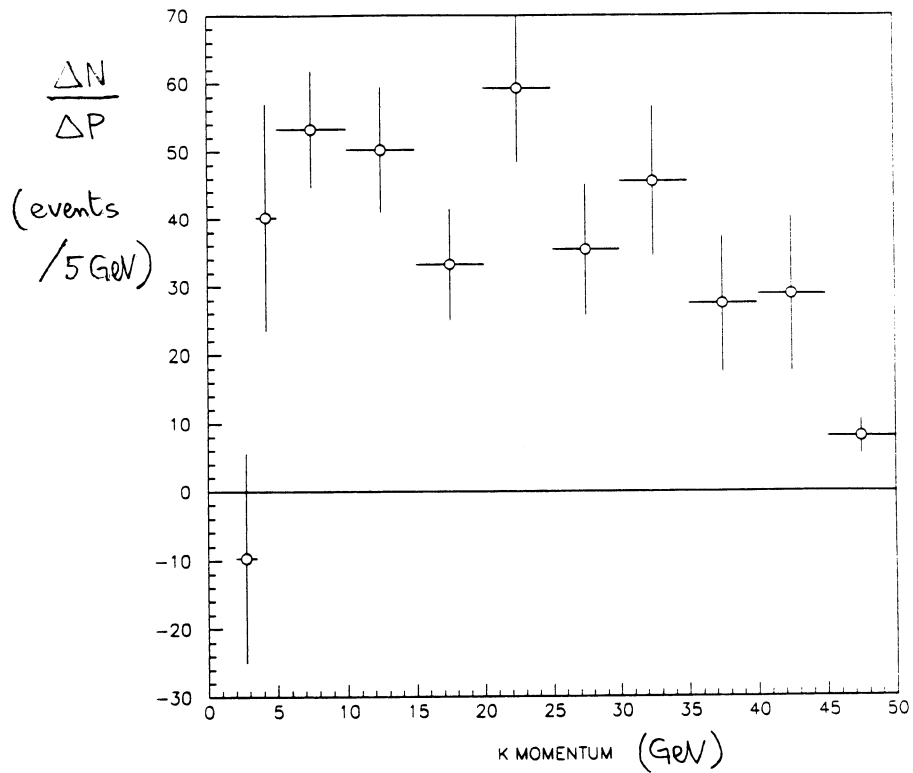
sample	$h$ inclusive	$h$	$h\pi^0$	$h2\pi^0$
events	28390	6764	11503	2788
$f_K(\%)$	$3.17\pm 0.14$	$5.85\pm 0.41$	$2.09\pm 0.19$	$0.90\pm 0.30$
$\chi^2/DF(dE/dx \text{ fit})$	1.3	1.0	1.1	0.9
$N_K$	$900\pm 40$	$396\pm 28$	$240\pm 22$	$25\pm 8$
channel	$\nu_\tau K \geq 0\pi^0 \geq 0K^0$	$\nu_\tau K$	$\nu_\tau K\pi^0$	$\nu_\tau K\pi^0\pi^0$
efficiency(%)	63.8	55.6	44.0	30.3
correction $\Delta N_K$	$+67\pm 24$	$-60\pm 22$	$-20\pm 8$	$-14\pm 4$
$B_K \pm \text{stat} \pm \text{syst}(\%)$	$1.58\pm 0.07\pm 0.12$	$0.63\pm 0.05\pm 0.05$	$0.52\pm 0.05\pm 0.07$	$0.04\pm 0.03\pm 0.02$



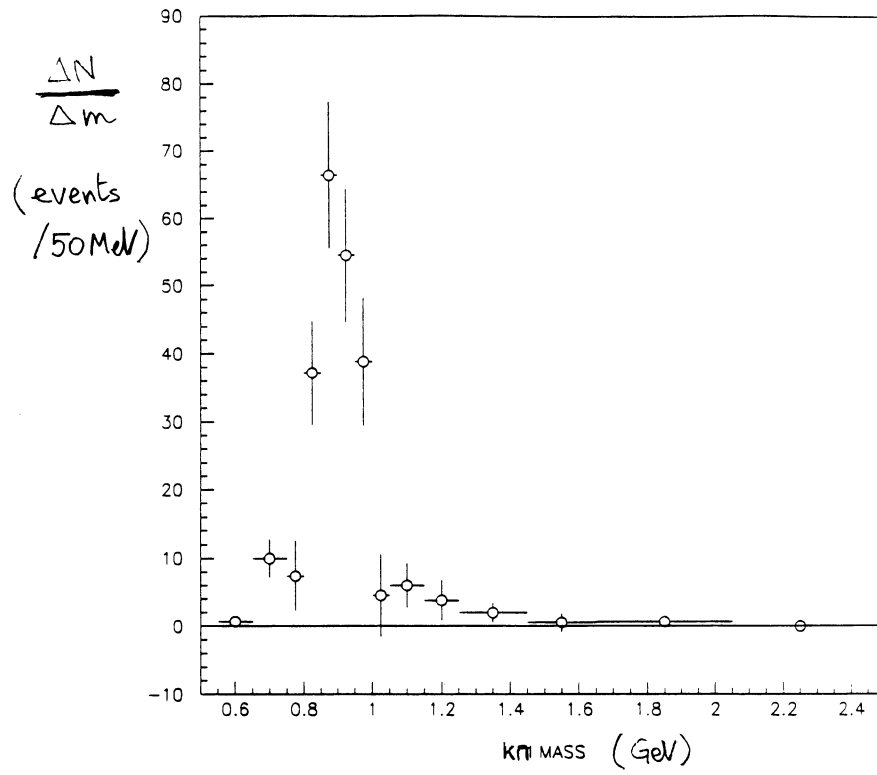
14. Inclusive  $K^-$  branching fraction [7].



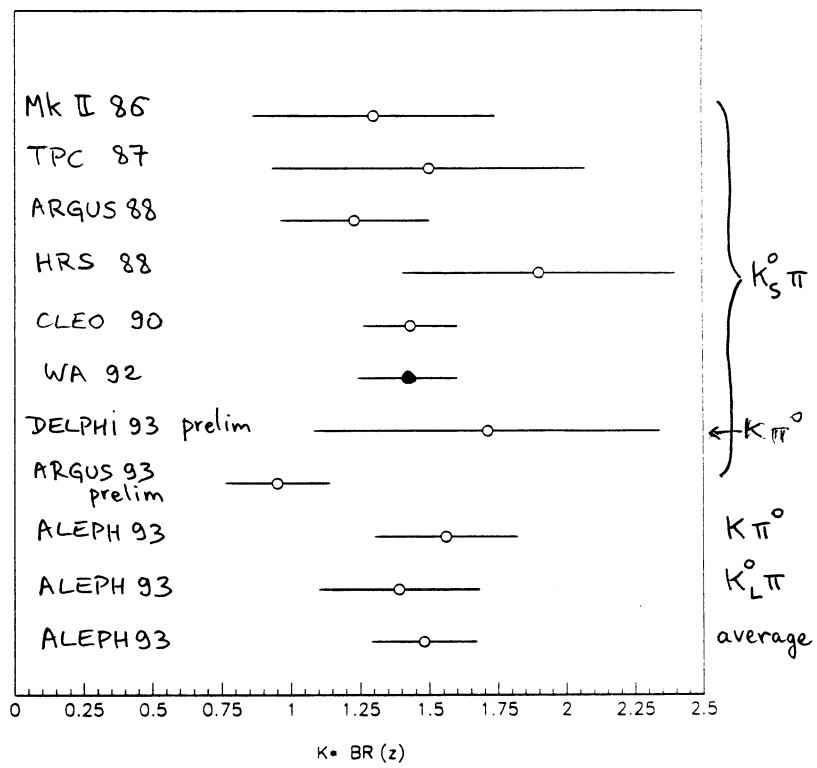
15.  $K$  branching fraction [7].



16. Momentum distribution of kaons in  $(\tau \rightarrow \nu_\tau K)$  decays.



17.  $K\pi^0$  mass distribution in  $(\tau \rightarrow \nu_\tau K\pi^0)$  decays.



18.  $K^*$  branching fraction [7].

The improvement in the single  $K$  channel (Fig.15) is even more significant (by a factor larger than 3) and for the first time a significant test of the Standard Model can be performed in the strange sector of the  $\tau$  (using  $B_e$  from ref. [4]) :

$$\frac{B(\tau^- \rightarrow \nu_\tau K^-)}{B(\tau^- \rightarrow \nu_\tau e^- \bar{\nu}_e)} = 0.035 \pm 0.004$$

to be compared to the value of 0.039 using  $\mu - \tau$  universality and the measured  $K \rightarrow \mu\nu$  decay rate.

Also, it is observed that the  $K$  momentum spectrum follows rather well the expected distribution including  $\tau$  polarization (Fig.16).

The  $\tau$  decay channel into  $\nu_\tau K\pi$  is expected to be dominated by  $K^*(892)$ . All the measurements so far have relied on the mode  $\pi^- K_S^0 (\rightarrow \pi^+ \pi^-)$ . The result given here on  $K\pi^0$  is consistent with the world average using  $K_S^0 \pi^-$  and has a similar accuracy. The  $K\pi^0$  mass distribution is indeed well described by the  $K^*$  resonance (Fig.17) and the other contributions taken from KORAL06. Correcting for all decay modes, one gets

$$B(\tau^- \rightarrow \nu_\tau K^{*-}) = (1.56 \pm 0.16 \pm 0.20)\%$$

The comparison with other experiments is given in Fig.18.

Finally, it is observed that the sum of the considered exclusive modes saturates the 1-prong inclusive  $K$  rate within the given accuracies, indicating that no other significant exclusive channel (with more  $\pi^0$ 's or more  $K^0$ 's) need to be considered at the 0.2% level

$$B_{K \text{ inclu}} - (B_K + B_{KK^0} + B_{K\pi^0} + B_{K\pi^0 K^0} + B_{K\pi^0 \pi^0}) = (0.05 \pm 0.13)\%$$

## 7 Summary

Using  $dE/dx$  information in the TPC, the 1-prong  $K$  decay rate of the  $\tau$  has been measured. Several exclusive modes have been identified and measured, four of them for the first time :

$$\begin{aligned} B(\tau^- \rightarrow \nu_\tau K^- \geq 0\pi^0 \geq 0K^0) &= (1.58 \pm 0.07 \pm 0.12)\% \\ B(\tau^- \rightarrow \nu_\tau K^-) &= (0.63 \pm 0.05 \pm 0.05)\% \\ B(\tau^- \rightarrow \nu_\tau K^- K^0) &= (0.29 \pm 0.12 \pm 0.03)\% \\ B(\tau^- \rightarrow \nu_\tau K^- \pi^0) &= (0.52 \pm 0.05 \pm 0.07)\% \\ B(\tau^- \rightarrow \nu_\tau K^- \pi^0 K^0) &= (0.05 \pm 0.05 \pm 0.01)\% \\ B(\tau^- \rightarrow \nu_\tau K^- \pi^0 \pi^0) &= (0.04 \pm 0.03 \pm 0.02)\% \\ \\ B(\tau^- \rightarrow \nu_\tau K^{*-}(892)) &= (1.56 \pm 0.16 \pm 0.20)\% \end{aligned}$$

# References

- [1] For a recent review, see M.Davier, Summary Talk of the 2nd International Workshop on  $\tau$  Lepton Physics, Colombus(Sept.92); Proceedings, K.K.Gan editor,1993
- [2] Review of Particle Properties, Phys.Rev. D45 (1992)
- [3] M.Davier and H.J.Park, ALEPH-note <sup>93-166</sup>, and F.Cerutti and L.Passalacqua, ALEPH-note in preparation
- [4] D.Decamp et al., ALEPH Coll., Z.Phys. C54 (1992)211
- [5] A new version of TAUPID with improved performances has been developed and will be described shortly in an ALEPH-note (M.Davier and H.J.Park). The earlier version and the general method are presented in : M.Davier and Z.Zhang, ALEPH-note 91-93
- [6] Z.Feng and R.Johnson, analysis meeting (Nov.92)
- [7] The preliminary 93 values are quoted in the review by A.Schwarz, Lepton-Photon Conference, Cornell (August 93)